OPEN ACCESS Freely available online

Journal of Geology & Geophysics

Research Article

Design and Analyse the Chemical Sensing for Optical Communication on Different Background Hexagonal PCF Using 2D FDTD Method

Nilambar Muduli[1*], **J S N Achary**[2], **Priya Sahu**[1], **Sibani Behera**[1]

[1]Department of Physics, Kalam Institute of Technology, Berhampur, Odisha, India; [2]Department of Physics, Ganjam College, Ganjam, Odisha, India

ABSTRACT

A novel high sensing circular and elliptical PCF are proposed based on selective glass material incorporation in the cladding region. By improving the structural parameter such as cladding diameter, pitch, core diameter, semi-major and semi-minor distance, angle of inclination, and eccentricity on the polarisation characteristics are fully discussed. A full vectorially 2D FDTD method with PML as boundary condition is applied and investigating guiding properties of proposed PCFs. Numerical simulations reveals that the proposed PCFs strongly effect on sensing response at a wavelength equal and greater than 1.55 μm. Additionally Confinement loss, mode field area and numerical apertures are significantly correlated to enhancing sensing arena. The results indicates that elliptical PCF has more sensing response over circular one at a wavelength equal to or greater than 1.55 μm, which is better than other reported literatures. Owing to above mentioned characteristics the proposed novel elliptical PCF can be widely applied in optical communication arena.

Keywords: PCF; Kerr-nonlinearity; Relative sensitivity; FDTD method

INTRODUCTION

Optical sensor devices have been taken as an alternative to conventional solid-state planar, brittle, less flexible, and rigid electronic devices [1]. Electronic devices have some major limitations such as high manufacturing cost, complex procedure, slower response time and reliability as compared to the optical sensors. Electronic devices are also affected with Electromagnetic (EM) and thermal noise or interference [2]. Now a day, physical sensing based on optical platform used to sense and monitor complex environment and its surrounding such as temperature, humidity, strain, stress, pressure, and torsion, etc. having important applications in wearable sensors, robotics, health and safety monitoring [3-8]. Therefore optical sensor devices have been found the suitable alternative for the gas, chemical and oil sensing applications, due to its advantages of low cost, less noise/interference, higher sensitivity, fast response, reliability, and compactness [9-11].

Since last decades, photonic crystal fiber has been shown great development in optical sensing [12-15]. Due to advance optical instrumentations, the field of fiber optics is no longer limited to telecommunication applications. PCF also known as holey fiber consists of periodically ordered microscopic cylindrical air holes running through the full length of the fiber. The standard PCF is made with fused-silica (SiO2) that has a regular pattern of voids or air holes that run parallel to its axis. Unlike traditional optical fibers, both the core and cladding are made from the same material.

Due to some inadequacy of conventional optical fibers, PCFs can be used to act as a sensor. The major shortcomings of conventional optical fibers are low index contrast narrow design space and high leakage loss. To control these difficulties, PCFs can be utilized. Photonic crystal fibers with various outlines of the opening example i.e. concerning the fundamental geometry of the cross section, the relative size of the gaps, and perhaps less relocation can have an exceptionally amazing property, unequivocally relying upon the configuration points of interest.

The sensing mechanisms of a PCF are absorbance that measured in a transparent medium, reflectance which is measured in non-transparent media, Luminescence based on the measurement of the intensity of light emitted by a chemical reaction in the receptor system, fluorescence, measured as the positive emission effect caused by irradiation, refractive index measured as the result of a change in solution composition, Opto-thermal effect based on a measurement of the thermal effect caused by light absorption, Light scattering based on effects caused by particles of definite size

Correspondence to: Nilambar Muduli, Department of Physics, Kalam Institute of Technology, Berhampur, Odisha, India, Tel: +9173810 54131; E-mail: nilambarmuduli00@gmail.com

Received: 03-Mar-2022; Manuscript No. JGG-22-16107; **Editor assigned:** 07-Mar-2022; PreQC. No. JGG-22-16107 (PQ); **Reviewed:** 21-Mar-2022; QC. No. JGG-22-16107; **Revised:** 28-Mar-2022; Manuscript No. JGG-22-16107 (R);**Published:** 04-Apr-2022, DOI: 10.35248/2381-8719.22.S4.002.

Citation: Muduli N, Achary JSN, Sahu P, Behara S (2022) Design and Analyse the Chemical Sensing for Optical Communication on Different Background Hexagonal PCF Using 2D FDTD Method. J Geol Geophys. S4:002.

present in the sample.

A chemical sensor is a device that transforms liquid sample information, ranging from the concentration of a specific sample component to the total composition analysis, into an analytically useful signal. The chemical information, may originate from a liquid reaction of the analyte or from a physical property of the system investigated. There are some applications of the chemical sensor. They are to perform Alcohol Breath Test, to detect toxic and flammable liquids which may cause fire/explosion and Environmental monitoring for safety measures [16-18].

Of evolution in 1996 changed fields such as telecommunication and sensing, leading to the inception of high sensitivity and restrained systems based on light conveyance. This phenomenal innate of fiber optics such as geometric adaptability, increased sensitivity over extant techniques. And inherent amity with fibre optic communication technology makes them stand out for sensing application. It is evident that the advantage of photonic crystal fiber over a conventional optical fiber depends on the size or geometrical configuration, modelling, band solving and different parametric properties. In fact sensors are reviewed as per their sensitivity variables. There is some basic ideas and example of current trend that can be investigated from this article on to the other future researches later. Henceforth there are various structural improvement of PCF sensor diverges from one another. In addition to this a large number of diverse structures can be assembled and these PCF sensors have significant criteria as compared to optical fiber and this can be facilitating the researchers and scientists later.

In this article, effect of sensing response incorporating the two configuration of PCF working with wavelength equal to or greater than 1550 nm has been investigated using 2D FDTD technique. We select typical PCFs in which the cross-section of cladding region is a solid core surrounded by circular and elliptical air holes of 5 layer hexagon array. In order to improve the sensing response of the PCF structure, we inserted the three liquid analyte such as water (n=1.33), ethanol (n=1.354) and benzene (n=1.366) for three background material PCF. This improved structure allows the x and y polarized mode to achieve in more distinct separation at the resonant frequency for sensing response. Furthermore the other PCF characteristics such as confinement loss, effective mode field area and numerical aperture can be calculated to enhance the sensing response at same wavelength range and compare them strictly between two proposed PCF. Our proposed configurations of PCF have the advantages of low cost, less noise, high sensitivity, fast response reliability, compactness in optical communication area.

MATERIALS AND METHODS

Mathematical analysis

In order to study the electric field profile pattern of proposed hexagonal PCF structures having elliptical and circular air hole in cladding region to be investigated and by implementing 2D-FDTD technique. Considering the material is isotropic, linear, and lossless, the time dependent Maxwell's equations can be written as

$$\frac{\partial H}{\partial T} = \frac{1}{\mu(\mathrm{r})}\nabla \times E \ldots(1)$$

$$H^{n+1/2}_{x(i,j)} = H^{n-1/2}_{x(i,j)} - \frac{c\Delta t}{\mu\Delta y}\left(E^{n}_{z\left(i,j+\frac{1}{2}\right)} - E^{n}_{z\left(i,--\frac{1}{2}\right)}\right)\ldots(2)$$

E, H are electric field and magnetic field.

Where ε(r), μ(r), σ(r) are permittivity, permeability and conductivity of the material and all are in the function of position.

Equations (1) and (2) can be discredited using Yee's technique. Considering spatial and time discretization, equations (1) and (2) can be written for TE polarization as follows:

$$H^{n+1/2}_{x(i,j)} = H^{n-1/2}_{x(i,j)} - \frac{c\Delta t}{\mu\Delta y}\left(E^{n}_{z\left(i,j+\frac{1}{2}\right)} - E^{n}_{z\left(i,--\frac{1}{2}\right)}\right)\ldots(3)$$

$$H^{n+1/2}_{y(i,j)} = H^{n-1/2}_{y(i,j)} + \frac{c\Delta t}{\mu\Delta x}\left(E^{n}_{z\left(i+\frac{1}{2},j\right)} - E^{n}_{z\left(i-\frac{1}{2},j\right)}\right)\ldots(4)$$

$$E^{n+1}_{z(i,j)} = E^{n}_{z(i,j)} + \frac{c\Delta t}{\varepsilon\Delta x}\left(H^{n+\frac{1}{2}}_{y\left(i+\frac{1}{2},j\right)} - H^{n+\frac{1}{2}}_{y\left(i-\frac{1}{2},\right)}\right) - \frac{c\Delta t}{\varepsilon\Delta y}\left(H^{n+\frac{1}{2}}_{x\left(i,j+\frac{1}{2}\right)} - H^{n+\frac{1}{2}}_{x\left(i,j-\frac{1}{2}\right)}\right)\ldots(5)$$

For stability, the time step $\Delta t \leq \frac{1}{c\sqrt{\Delta x^{-2} + \Delta y^{-2}}}$ where Δt the time increment, c is the velocity of light,Δx be the lattice increment in x direction, Δy be the lattice increment along y direction.

Considering equation (3), (4) and (5), we have calculated the field distribution of PCFs in TE polarization mode.

For a nonlinear optical waveguide having Kerr-type non-linearity related permittivity ε_r depends on electric field E_y and can be expressed as

$$\varepsilon_r = \varepsilon_{r.L} + \alpha\left|E_y\right|^2 \ldots(6)$$

Where $\varepsilon_{r.L}$ is the linear relative permittivity and α is the non-linear co-efficient. A hybrid implicit FDTD method is used to simulate the field for 2D PCS with nonlinear rods. The overall stability of this hybrid FDTD scheme is determined by the stability in the linear medium regions. Consequently, nonlinearity in the structure does not affect stability and hence the grid size and time step.

The cladding region consists of finite number of air holes so it may cause the leakage of light. This leakage of light from core to exterior material results the confinement loss (dB/km) that can be expressed as:

Confinement loss = $8.686k_0I_m$ [n_{eff}] dB/km ...(7)

Where I_m is the imaginary part, n_{eff} is the effective index of x polarized and y polarized fundamental mode.

The relative sensitivity coefficient measures the interaction between the light and the analyte to be sensed. This interaction is measured through the absorption coefficient at a particular wavelength. According to the Beer-Lambert law, light is attenuated by the intensity of absorption of evanescent wave [17].

$I(\lambda) = I_0(\lambda)\exp[-r\alpha_m l_c]$ ...(8)

The absorbance of the sample to be detected is defined by the following equation:

$A = \log\left(\frac{I}{I_o}\right) = r\,\alpha_m\,l_c$ ...(9)

Where I and I0 are the input and output intensities, respectively, and c is the concentration of absorbing material. The length of the channel is l. The function of absorption coefficient is $\alpha_m(\lambda)$, and r is the relative sensitivity coefficient, which can be defined by the following equation [18].

$$r = \frac{n_r}{n_{eff}} f \ldots(10)$$

where nr refers to the refractive index of the sample to be sensed, and n_{eff} is the effective index of the guided mode, f is the fraction of total power located in the core, and it is also known as a power distribution function [19] by using Poynting's theorem which can be expressed as the following equation:

$$f = \frac{\int Re\left(E_x H_y - E_y H_x\right)dxdy}{\int Re\left(E_x H_y - E_y H_x\right)dxdy} \times 100 \ldots(11)$$

Where numerator integration for sample and denominator integration for total. Where E_x and H_x are transverse electric field and respectively; E_y and H_x are longitudinal electric field and magnetic field respectively. The f measures the % of energy which present in the holes.

The effective mode field area A_{eff} (μm^2) and the Numerical Aperture (NA) of the fiber is evaluated as follows:

$$A_{eff} = \frac{\left(\iint |E|^2\, dxdy\right)^2}{\iint |E|^4\, dxdy} \ldots(12)$$

$$NA = \left(1 + \frac{\pi A_{eff}}{\lambda^2}\right)^{-1/2} \ldots(13)$$

PCF design

In order to obtain the chemical sensing response of purposed PCF structures, the transverse cross-sectional view of such PCF structure has been illustrated in Figure 1. It consists of an array of circular and elliptical air hole arranged in a triangular lattice pattern in different background material PCF.

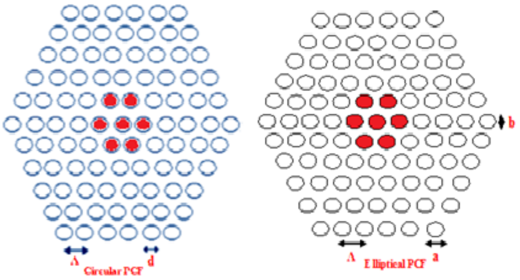

Figure 1: The Cross-sectional view of proposed circular and elliptical PCF.

It is very essential that to fabricate number of air holes for maintain the responsibility of dielectric medium. PCFs having different background material whose cladding region is composed of air hole ring constructed with circular, elliptical pattern. Choosing 'd' be the diameter of air hole for circular PCF cladding region and a, b are the semi major and semi minor axis of elliptical background PCF. Pitch is set to be $\frac{d}{0.93}$ μm and the core segments of proposed PCFs have been circular and elliptical air holes with 45° orientation. We set 'a' and 'b' are the semi major and semi minor distance of ellipse with eccentricity e=0.6. For liquid infiltration refractive index of core region are always greater than cladding region and light propagation through PCFs due to total internal reflection phenomena.

RESULTS AND DISCUSSION

The effects of the fiber structural parameter on its polarisation characteristics have been investigated in above section. We compare the different of circular and elliptical PCF filled with liquid analyte being estimated. Figure 2 shows the electric field distribution pattern of X and Y polarisation of proposed PCFs which operated at a wavelength of 1.55 μm, The simulation picture nicely shown that light almost tightly confined in fluoride glass and silica based PCF structure while light spread out in the vicinity of cladding region in case of BK7 background based PCF. In addition, it is seen that circular PCFs may less concern for sensing response over elliptical PCF even though fabrication of elliptical PCF being very difficult.

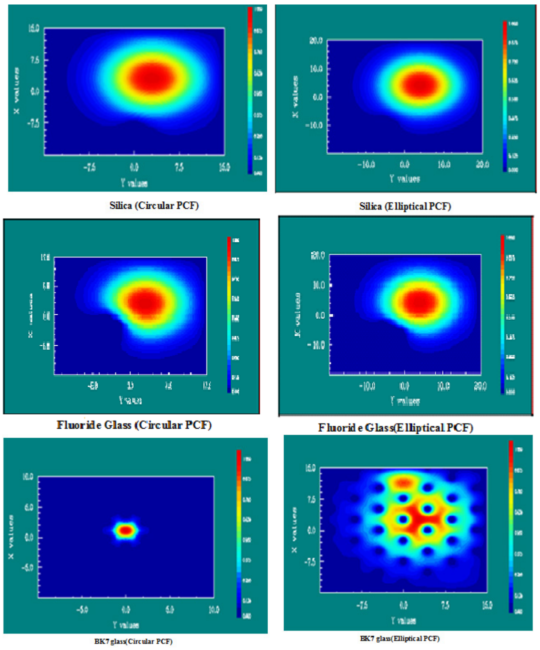

Figure 2: Field distribution of design for circular and elliptical PCF of three different background material (Silica Fluoride glass BK7 glass) at operating wavelength of 1.55 μm for ncore=1.354.

The first and foremost nature of PCF used as sensor is needed to compute the relative sensitive response. This sensitivity response of a PCFs denoted that the sensing capacity of the proposed PCFs. For the first time, we have computed the sensitivity response of various liquid analyte such as water ethanol and benzene respectively on the basis of refractive index. The refractive index can be evaluated based on wavelength range using Sellimeir equation (not shown here). Figure 3a illustrates the relative sensitivity on wavelength range for water when the background material are chosen to be silica Fluoride glass and BK7. it is seen that the relative sensitivity gradually increase with increasing wavelength in both PCF structure The result clearly revealed that the available sensitivity values are 60.2%, 61.6% and 61.7% offered by BK7, silica and Fluoride glass circular PCF while 60.7%, 62.2% and 62.3% by elliptical PCF at an operating wavelength of 1.55 μm. As illustrated in above figure the loss of sensing response in circular proposed PCF is greatly affected by diameter of air hole rings over elliptical PCF. Hence the sensitive response result is better in elliptical PCF over circular one. However Figures 3b and 3c predicts that the relative sensitivity on wavelength range of ethanol and benzene analyte for three background material PCF. The sensitivity result simultaneously obtained are 60.8%, 62.3% and 62.4% for ethanol which operated at a wavelength of 1.55 μm of proposed circular PCF while 61.3%,62.7% and 62.8% for elliptical PCF. At the same time, benzene analyte offers the sensitivity values are 61.0%, 62.7%and 62.8% for proposed circular PCF however the elliptical PCF shows relative sensitivity of 61.8%, 63.7% and 64%. From above result, it concludes that Fluoride glass shows better enhancing their sensing response over silica and BK7 at an operating wavelength of 1.55 μm. Hence it is most extensively suitable glass material in sensing arena.

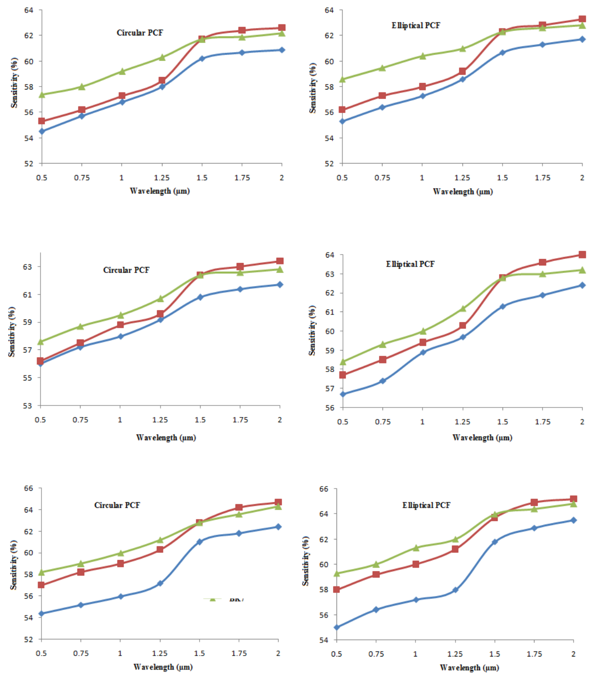

Figure 3: Sensitivity versus Wavelength for three different PCF background material for. a) n=1.33 b) n=1.354 c) n=1.366. **Note:** (-◆-) Silica; (-■-) Fluorlde glass; (-▲-) BK7

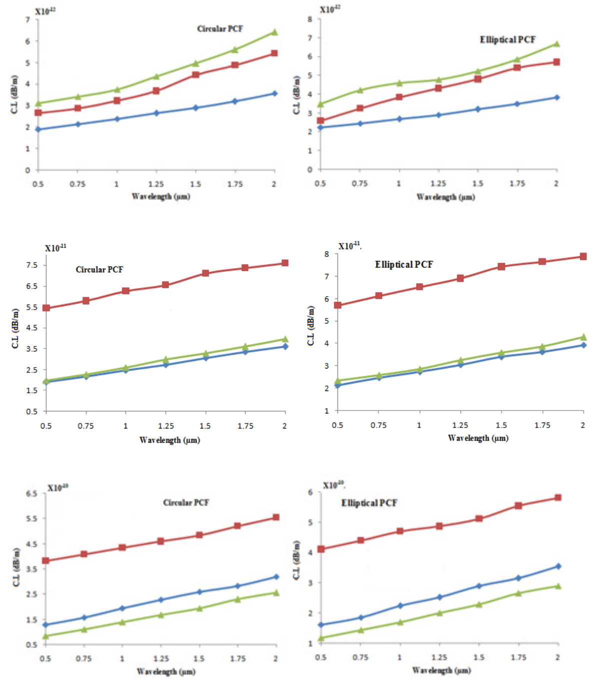

Figure 4: Confinement Loss versus Wavelength for three different PCF background material for. a) n=1.33 b) n=1.354 c) n=1.366. **Note:** (-◆-) Silica; (-■-) Fluorlde glass; (-▲-) BK7

While making fabrication of our proposed PCF, the confinement loss is the most vital key role in optical communication arena. It occurs due to the leaky nature of the mode and irregular arrangement of air holes. These air holes are playing the role of dielectric medium and it depends also on transmitted wavelength, parameter shape and size, number of air holes rings. It is evident that, more light energy is confined in the fiber core which produces less confinement loss, hence it is very essential to evaluate the confinement loss.

Figure 4 represent the variation of confinement loss on wavelength of proposed PCF for different sensing liquid analytes. It is noticeable that, the confinement loss curve gradually increases on increasing in wavelength for all three liquid analyte of proposed PCF. It is seen that, Figures 4a-4c confinement loss slightly more for Fluoride glass and BK7 over the silica while Figure 4a shows that the confinement loss is more for BK7 over fluoride glass and silica. However from the Figure 4, we can see clearly from the improved structure that elliptical PCF structures show better result over circular one.

Mode field area (A_{eff}) is one of the most important parameter of PCF for high bit rate communication at high power transmission. The main function of mode field area to transmit data in an optical system. Hence it is very essential to estimate the effective mode field area for different background material PCF. Figure 5 represent the variation of effective mode field area on wavelength for different values refractive index of liquid analyte which potential to allow enhancing sensing response. It is viewed from Figure 5a that the value of mode field area of BK7 is more than Fluoride glass below the operating wavelength of 1.55 µm. But Fluoride glass has more mode field area above the same operating wavelength. Additionally, A_{eff} of Silica is reduced value over BK7 and Fluoride glass. On the other hand in Figures 5b and 5c clearly indicate that, Fluoride glass is the most prominent glass material which attain maximum A_{eff}. Furthermore, Fluoride glass has somehow more A_{eff} value attained in elliptical PCF than circular one. Henceforth fabrication of elliptical PCF is very crucial and measure accurate result for optical communication arena over the circular one.

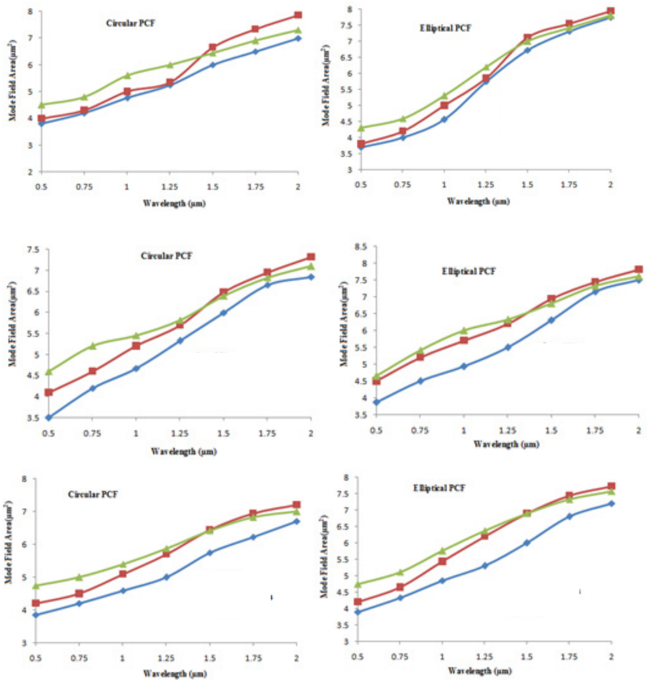

Figure 5: Mode field area versus Wavelength for three different PCF background material for. a) n=1.33 b) n=1.354 c) n=1.366.. **Note:** (-◆-) Silica; (-■-) Fluorlde glass; (-▲-) BK7

The another characteristics of PCF as NA which is also much more important for sensing arena, It is a measure of ability of an optical fiber to collect or confine the incident light inside it and capable to accept maximum light. In fact, more is the NA; the fiber gathers more light, so it is quite essential to measure the NA for proposed PCFs based sensor which initiated in chemical or bio-sensing purpose. Figure 6 demonstrate the NA on wavelength of different refractive index based liquid analyte.

Finally it is clarified that, NA decreases with increasing wavelength, The NA curve indicates that BK7 glass elliptical PCF has more value than silica and fluoride glass, e.g NA is more in elliptical PCF than circular one for all three types of background material. While it is very interesting result obtained as NA value is almost constant for all glass material, e.g it has the average value of 2.66 for elliptical PCF and 2.48 for circular PCF at an operating wavelength of 1.55 µm. However NA increases with increasing wavelength hence the curve for BK7 is greater than silica and fluoride glass. But now we measure that BK7 always shows better NA than silica and fluoride glass which shown in below Table 1.

In this article, the full vectorially 2D FDTD method based numerical studies have been reported. Our results are expected to suggest some valuable reference to design the proposed PCF in sensing application. In fact the fabrication of PCF structure being comparatively very simple, so several methods like stack and draw, extrusion, air hole drilling and sol gel technique have offered any types of structure. However by recent development technology, the proposed design can be fabricated for technological improvement in the fabrication of PCFs. In this article, the proposed PCFs can be fabricated by the air hole drilling method.

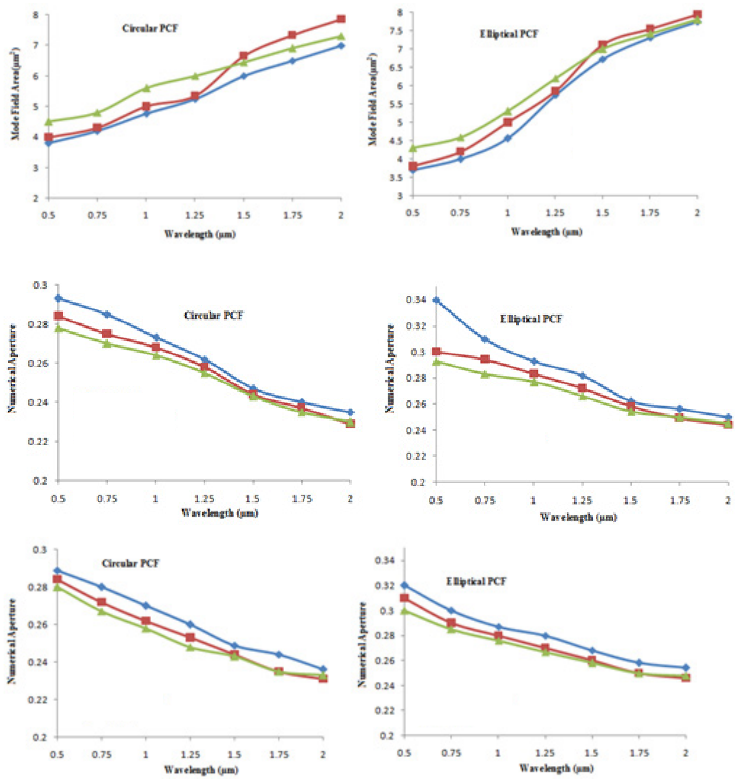

Figure 6: Numerical Aperture versus Wavelength for three different PCF background material for. a) n=1.33 b) n=1.354 c) n=1.366. **Note:** (-◆-) Silica; (-■-) Fluorlde glass; (-▲-) BK7

Table 1: Analysis of different background material based on circular and elliptical PCF sensor at an operating wavelength of 1.55 µm.

Background	Core (R.I)	Sensitivity (%)		C.L (dB/m)		Aeff (µm2)		NA	
		C-PCF	E-PCF	C-PCF	E-PCF	C-PCF	E-PCF	C-PCF	E-PCF
Fluoride glass	n=1.33	61.7	62.3	4.43*10-12	4.80*10-12	6.65	7.125	0.243	0.26
	n=1.354	62.4	62.8	7.1*10-11	7.42*10-11	6.48	6.95	0.244	0.258
	n=1.366	62.8	63.7	4.84*10-10	5.12*10-10	6.45	6.9	0.245	0.26
Silica	n=1.33	61.6	62.2	2.89*10-12	5.32*10-12	6.44	6.725	0.24	0.26
	n=1.354	62.3	62.7	3.06*10-11	3.4*10-11	6.4	6.8	0.243	0.254
	n=1.366	62.7	64	2.60*10-10	2.90*10-10	6.42	6.9	0.244	0.258
BK7	n=1.33	60.2	60.7	5.60*10-12	5.64*10-12	6	7	0.248	0.268
	n=1.354	60.8	61.3	3.28*10-11	3.59*10-11	6	6.3	0.247	0.262
	n=1.366	61	61.8	1.95*10-10	2.29*10-10	5.57	6	0.249	0.268

CONCLUSION

We propose a high sensing PCFs based on the introduction of elliptical and circular air holes with a specific position distribution around the core. We choose two proposed PCF with three background material (Fluoride glass, silica and BK7) for their investigation. In addition, we also investigated that the liquid analyte such as water (n=1.33), ethanol (n=1.354) and benzene (n=1.366) are filled in a single layer core for sensing response. The sensing properties of the specific modes are investigated comprehensively using 2D FDTD method, such property of circular and elliptical PCF are also compared and estimated. Moreover the sensing property can be enhanced by incorporating close approximate to confinement loss, effective mode field area and numerical aperture of proposed PCFs. It is seen that, fluoride glass elliptical shows better performance on sensitive response over circular one than silica and BK7 PCF even though the fabrication of elliptical PCF being very difficult. They are in order as SF.g>SSi>SBk7 at a wavelength equal to or greater than 1.55 μm range and is applicable for optical communication purpose.

AVAILABILITY OF DATA AND MATERIAL

The data that support the findings of this study and the raw data of each figure in this manuscript are accessible through literature survey.

ACKNOWLEDGEMENT

The authors are grateful to those who have participated in this research work.

REFERENCES

1. Xu K, Lu Y, Takei K. Multifunctional skin-inspired flexible sensor systems for wearable electronics. Adv Mat Technol. 2019;4(3):1800628.
2. Correia R, James S, Lee SW, Morgan SP, Korposh S. Biomedical application of optical fibre sensors. J Optic. 2018;20(7):073003.
3. Liu Y, Salemink HW. All-optical on-chip sensor for high refractive index sensing in photonic crystals. EPL. 2014;107(3):34008.
4. Yeo JC, Lim CT. Emerging flexible and wearable physical sensing platforms for healthcare and biomedical applications. Microsyst Nanoeng. 2016;2(1):1-9.
5. Miao P, Wang J, Zhang C, Sun M, Cheng S, Liu H. Graphene nanostructure-based tactile sensors for electronic skin applications. Nano-Micro Let. 2019;11(1):1-37.
6. Costa JC, Spina F, Lugoda P, Garcia-Garcia L, Roggen D, Münzenrieder N. Flexible sensors—from materials to applications. Technol. 2019;7(2):35.
7. Almassri AM, Wan Hasan WZ, Ahmad SA, Ishak AJ, Ghazali AM, Talib DN, Wada C. Pressure sensor: State of the art, design, and application for robotic hand. J Sensor. 2015.
8. Zou M, Ma Y, Yuan X, Hu Y, Liu J, Jin Z. Flexible devices: From materials, architectures to applications. J Semiconduct. 2018;39(1):011010.
9. Asaduzzaman S, Paul BK, Ahmed K. Enhancement of sensitivity and birefringence of a gas sensor on micro-core based photonic crystal fiber. In 2016 3rd ICEEICT .IEEE. 2016;1-4.
10. Triyana K, Rianjanu A, Nugroho DB, As'ari AH, Kusumaatmaja A, Roto R, et al. A highly sensitive safrole sensor based on polyvinyl acetate (PVAc) nanofiber-coated QCM. Scient Rep. 2019;9(1):1-2.
11. Cui S, Wang J, Wang X. Fabrication and design of a toxic gas sensor based on polyaniline/titanium dioxide nanocomposite film by layer-by-layer self-assembly. RSC Adv. 2015;5(72):58211-58219.
12. Ju J, Jin W. Photonic crystal fiber sensors for strain and temperature measurement. J Sensor.2009.
13. Pinto AM, Lopez-Amo M. Photonic crystal fibers for sensing applications. J Sensor. 2012.
14. Argyros A. Structure, properties and characteristics of optical fibres. In Handbook of textile fibre structure. Woodhead Pub. 2009:458-484.
15. Zografopoulos DC, Pitilakis A, Kriezis EE. Liquid crystal-infiltrated photonic crystal fibres for switching applications. Optofluid Sensor Actuat Microstruct Opt Fiber. 2015:55-83.
16. Riyadh SM, Hossain MM, Mondal HS, Rahaman ME, Mondal PK. Photonic Crystal Fibers for Sensing Applications. J Biosens Bioelectron. 2018;9:251.
17. Ademgil H, Haxha S. PCF based sensor with high sensitivity, high birefringence and low confinement losses for liquid analyte sensing applications. Sensor. 2015;15(12):31833-31842.
18. Johny J, Prabhu R, Fung WK. Investigation of structural parameter dependence of confinement losses in PCF–FBG sensor for oil and gas sensing applications. Opt Quantum Electron. 2016;48(4):1-9.